UNIVERSITE DE BOURGOGNE
U.F.R. Sciences et Techniques
Filière : **Master 2 CMPP**

Année 2012-2013
22 janvier 2013

Session : **1**

EPREUVE :
Electrochimie

Durée : 01h00

I - A quelle problématique répond le concept de *catalyse moléculaire de réactions électrochimiques* ? A quoi est-elle une alternative ?
Représenter le schéma de principe et en décliner les avantages.
Distinguer les modes par *catalyse redox* et *catalyse chimique*.

II - **Analyse de publication :** *Chemistry – A European Journal* **2012**, *18*, 6581-6587

1. Décrivant le voltammogramme cyclique du composé **3**, en l'absence de base ajoutée, l'auteur de l'article écrit : « ... *a reversible one-electron wave was observed* ... ».
a) Enoncer les différents critères et leur valeur permettant de qualifier ainsi la réponse voltammétrique.
b) Selon le pic considéré, dire la transformation redox s'effectuant à l'électrode sur la base des différentes espèces représentée sur le schéma 2.

2. Envisageons maintenant la courbe f (courbe en traits pointillés sur la figure 1), obtenue par addition d'un large excès de base (imidazole) sur le composé **3**.
a) En relation avec le mécanisme du schéma 2, expliquer l'incidence de l'addition de la base sur la réaction d'oxidation.
b) Même question qu'en 1.b). Indiquer le nombre d'électrons transférés à chaque stade.

3. Examinons maintenant le voltammogramme de la figure 2.
a) Quel paramètre d'expérience, fondamental en voltammétrie cyclique, a été changé par rapport aux conditions de la figure 1 ?
b) Sur la figure 2, quel pic supplémentaire peut-on observer (sur la courbe b, par exemple) et de quelle espèce est-il l'expression ?

4. Le voltammogramme I de la figure 3 se différencie par la forme de la courbe obtenue (par opposition, par exemple, au voltammogramme cyclique a de la figure 1).
a) Si, en voltammétrie cyclique, le régime de diffusion est dit *variable*, comment le qualifier pour le voltammogramme I de la figure 3 ? Présentement, par quelles conditions expérimentales, obtient-on ce régime ?
b) Pour ce voltammogramme I, la réponse est mono-électronique et réversible (ou nersntienne). Quelles sont les caractéristiques quantitatives associées à un tel système ?

5. Au stade du voltammogramme I de la figure 3, est réalisée une électrolyse.
a) Préciser les éléments les plus essentiels du dispositif. Sous quelle configuration se trouve la cellule et quel est le paramètre contrôlé par l'opérateur ?
b) Préciser les réactions aux électrodes.

DOI: 10.1002/chem.201103378

Deciphering the Activation Sequence of Ferrociphenol Anticancer Drug Candidates

Pierluca Messina,[a] Eric Labbé,*[a] Olivier Buriez,[a] Elizabeth A. Hillard,[b] Anne Vessières,[b] Didier Hamels,[b] Siden Top,[b] Gérard Jaouen,[b] Yves Michel Frapart,[c] Daniel Mansuy,[c] and Christian Amatore*[a]

Abstract: The complete oxidation sequence of a model for ferrociphenols, a new class of anticancer drug candidate, is reported. Cyclic voltammetry was used to monitor the formation of oxidation intermediates on different timescales, thereby allowing the electrochemical characterization of both the short-lived and stable species obtained from the successive electron-transfer and deprotonation steps. The electrochemical preparation of the ferrocenium intermediate enabled a stepwise voltammetric determination of the stable oxidation compounds obtained upon addition of a base as well as the electron stoichiometry observed for the overall oxidation process. A mechanism has been established from the electrochemical data, which involves a base-promoted intramolecular electron transfer between the phenol and the ferrocenium cation. The resulting species is further oxidized then deprotonated to yield a stable quinone methide. To further characterize the transient species successively formed during the two-electron oxidation of the ferrociphenol to its quinone methide, EPR was used to monitor the fate of the paramagnetic species generated upon addition of imidazole to the electrogenerated ferrocenium. The study revealed the passage from an iron-centered to a carbon-centered radical, which is then oxidized to yield the quinone methide, namely, the species that interacts with proteins and so forth under biological conditions.

Keywords: antitumor agents · cyclic voltammetry · ferrociphenols · oxidation · reaction mechanisms

Results and Discussion

Base-dependent electrochemical behavior of compound 3: The oxidation of **3** in the presence of increasing amounts of imidazole was investigated by cyclic voltammetry (CV) in acetonitrile (Figure 1). In the absence of imidazole (curve a), a reversible one-electron oxidation wave was observed at 0.39 V that was ascribed to the oxidation of the ferrocene moiety, as already established for other ferrociphenols.[12,14,16] Upon addition of imidazole, the intensity of the oxidation wave dramatically increased and progressively split, leading ultimately to two distinct peaks at large imidazole excesses (curves e and f). The first wave displayed a potential dependence with imidazole concentration, and shifted towards less positive potential within a window of approximately 120 mV from curve a to curve f. Its intensity was 2.2 times higher than that of curve a, which corresponds to the passage from a mono- to a bielectronic wave.[21] The second wave observed at approximately 0.46 V remained reversible independently of the imidazole excess and was monoelectronic (by comparison with curve a).

The electrochemical behavior of compound **3** strongly suggests that the first base-dependent bielectronic wave represents the oxidation of **3** into the quinone methide **3d**. This

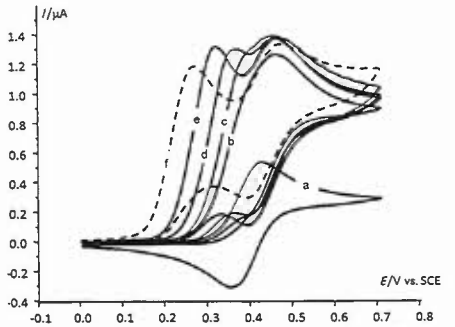

Figure 1. Cyclic voltammograms of **3** (0.9 mM) in acetonitrile/$TBABF_4$ (0.1 M) with increasing concentration of imidazole: a) 0, b) 0.9, c) 4.5, d) 18, e) 90, and f) 560 mM (dashed curve). Electrode: Pt, 0.5 mm diameter; scan rate: 100 $mV s^{-1}$.

assumption is consistent with the exchange of two electrons and two protons required to convert **3** to **3d**. This base-dependent potential shift could be interpreted by either considering the intrinsic acidity constants of the proton donor (phenol) and the acceptor (imidazole) or taking into account the hydrogen-bonding interactions between the same species, as highlighted for the reciprocal reduction of quinones.[22] However, compound **3** is the only ferrociphenol exhibiting such a dramatic base dependence in the voltammograms, which suggests that the pre-formation of a base complex by hydrogen bonding—which is expected in the phenol series—did not play a major role in the oxidation process, so deprotonation remained bimolecular. This observation contrasts with the behavior of other ferrociphenols and is certainly due to the steric constraints imposed by the two methyl *ortho* substituents.[23,24] Therefore, considering the more acidic character of cresols/resorcinols versus phenols,[20] the intrinsic acidity of **3**, enhanced in its cation radical—which is a boundary mesomeric structure of the ferrocenium cation $3^{\bullet+}$ (Scheme 2)[23]—should play the major role in the energetics and kinetics of this base-promoted oxidation sequence. The second monoelectronic wave can be assigned to the oxidation of the ferrocene moiety of **3d** (forming $3d^+$), which means that at high imidazole excesses and at low scan rates, the overall bielectronic oxidation of **3** is fast enough to allow the observation of the oxidation of **3d** to $3d^+$ within the same CV scan.

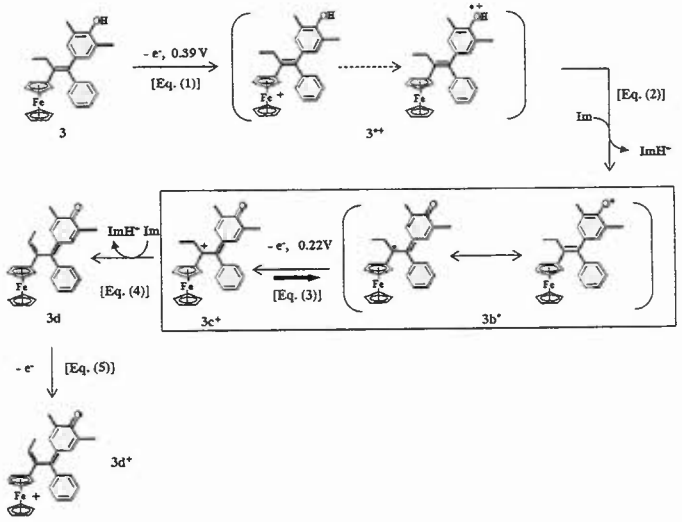

Scheme 2. Full oxidation sequence of ferrociphenol 3.

Electrochemical behavior during shorter time intervals: Figure 2 displays the cyclic voltammograms of **3** at 75 Vs^{-1} in the presence of various excess amounts of imidazole.

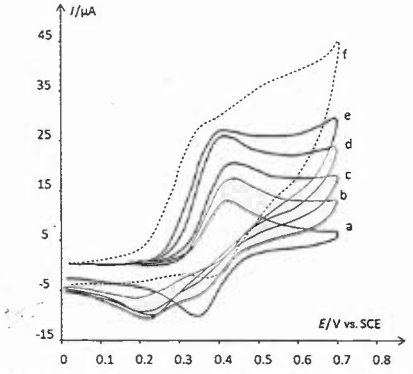

Figure 2. Cyclic voltammograms of **3** (0.9 mM) in acetonitrile/$TBABF_4$ (0.1 M) with increasing concentration of imidazole: a) 0, b) 0.9, c) 4.5, d) 18, e) 90, and f) 720 mM (dashed curve). Electrode: Pt, 0.5 mm diameter; scan rate: 75 Vs^{-1}.

pectedly, in the 5–100 equiv range of excess amounts of imidazole, a new reduction peak was observed at 0.22 V on the reverse scan. This reduction peak first increased with the imidazole concentration and reached a maximum at 20 equiv, then decreased (becoming vanishingly small at 800 equiv). Since no reduction process was observed at 100 mVs^{-1} in the 0.2–0.3 V region, this new reduction wave could be ascribed to a transient species observable only at fast scan rates. Indeed, the time window corresponding to the generation of the oxidized compounds in the forward scan (which starts at approximately 0.35 V) and the reduction at 0.22 V in the backward scan was in the 10 ms range for the voltammograms in Figure 2. Moreover, the transient species reduced at 0.22 V was only observed with intermediate excess amounts of imidazole, which suggests that it was not formed at low imidazole concentrations, but had fully evolved under large excess amounts. This identifies a new intermediate, the formation and conversion of which is both time- and base-dependent. It is unlikely that a ferrocenium species is reduced at 0.22 V, since the Fc/Fc^+ systems of the phenol and quinone are observed in the 0.4–0.5 V range. Therefore, the reduction at 0.22 V must feature a later species formed after the deprotonation of $\mathbf{3}^{\bullet+}$. With respect to these considerations, the cathodic wave observed at 0.22 V most likely corresponded to the reduction of a carbocation obtained after the one-electron oxidation of radical **3b**, as reported in Scheme 2. Such an interpretation is fully coherent with the mechanism in Scheme 2 whenever the first deprotonation (that is of the phenol cation radical) is faster than that of the carbocation formed after the second oxidation.

Hence, with large excess amounts of imidazole and/or longer timescales, this cation is fully deprotonated to afford the quinone methide **3d**, and its reduction may not be observed any longer. At lower imidazole concentrations and/or shorter time windows, the carbocation has a sufficient lifetime so that its reduction may be observed during the backward voltammetric scan. At even lower imidazole concentrations or faster scan rates, the first deprotonation cannot proceed, thus the carbocation cannot be formed. Only a very tiny window of time and imidazole concentration may allow the observation of this transient intermediate. In previous investigations, the conversion of the carbon-centered radical to the quinone methide could be evidenced only through its overall reaction. With **3**, the relative reactivities of $\mathbf{3}^{\bullet+}$ and $\mathbf{3c}^+$ allowed the observation of the electrochemical signature of $\mathbf{3c}^+$, a fact that further validates the oxidation mechanism of phenol-substituted ferrocifen compounds in Scheme 1.

Stepwise electrolyses of 3: Electrolyses of **3** were carried out in acetonitrile. Steady-state voltammetry at a UME was used to monitor the concentrations of the species at various electrolysis stages.

In the absence of imidazole, one can observe in Figure 3 the one-electron oxidation of **3** (curve I). In the absence of imidazole, a 0.95 $Fmol^{-1}$ electrolysis of **3** changed the solution from pale yellow to red and gave a new voltammogram (curve II). The color change, together with the approximately quantitative consumption of the original species at 0.95 $Fmol^{-1}$ was consistent with the conversion of **3** into $\mathbf{3}^{\bullet+}$. The subsequent addition of a tenfold molar excess of imidazole to the solution obtained after the electrolysis (curve II) triggered the reaction sequence presented in Scheme 2. The corresponding steady-state voltammogram (curve III) no

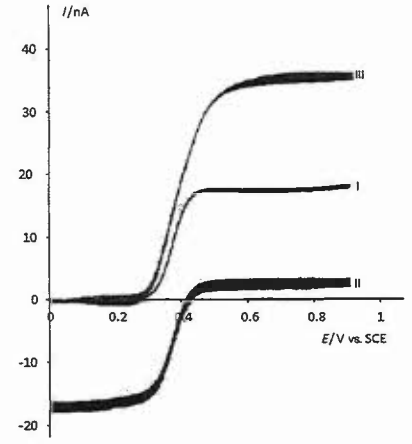

Figure 3. Steady-state voltammograms of acetonitrile/$TBABF_4$ (0.1 M) solutions containing I) compound **3** (5 mM); II) solution I after 0.95 Faraday mol^{-1} electrolysis at 0.7 V; and III) solution II after addition of imidazole (50 mM). Electrode: Pt, 25 μm diameter; scan rate: 20 mVs^{-1}.

longer displayed a reduction process but roughly featured an overall two-electron oxidation process by comparison with curve I. Actually, the radical species $\mathbf{3b}^{\bullet}$ formed after imidazole addition to $\mathbf{3}^{\bullet+}$ could be oxidized in an homogeneous way by $\mathbf{3}^{\bullet+}$, since the voltammograms in Figures 1 and 2 clearly show that the radical intermediate was easier to oxidize than the original ferrociphenol **3**. In that case, the redox reaction should be written as shown in Equation (6):

$$\begin{aligned} &\mathbf{3}^{\bullet+} + \mathrm{Im} \rightarrow \mathbf{3b}^{\bullet} \\ &\mathbf{3}^{\bullet+} + \mathbf{3b}^{\bullet} \rightarrow \mathbf{3} + \mathbf{3c}^{+} \\ &\mathbf{3c}^{+} + \mathrm{Im} \rightarrow \mathbf{3d} \\ &\text{Overall}: \; 2(\mathbf{3}^{\bullet+}) + 2\,\mathbf{Im} \rightarrow \mathbf{3} + \mathbf{3d} \end{aligned} \qquad (6)$$

The chemical sequence triggered upon addition of imidazole to $\mathbf{3}^{\bullet+}$ followed a complex mechanism that ultimately led to the formation of **3** and **3d** as the stable species, their oxidation being globally bielectronic in curve III. In summary, these stationary voltammograms show that the sequence observed on the timescale of cyclic voltammetry (that is, a few seconds) in Figure 1 is still valid during a time period corresponding to preparative electrolysis, typically 5–15 min.

We have further characterized by ^1H and ^{13}C NMR spectroscopy the species formed after the bielectronic oxidation of **3** in the presence of imidazole. The spectra displayed signals that could be clearly ascribed to the quinone methide $\mathbf{3d}$[17] (see the Supporting Information).

Experimental Section

Reagents: Acetonitrile was purchased from Acros Chemicals (extra dry) and used as the solvent without further purification. Tetrabutylammonium tetrafluoroborate ($TBABF_4$) used as the supporting electrolyte was prepared from $NaBF_4$ (Acros) and nBu_4NHSO_4 (Acros), recrystallized from ethyl acetate/hexane (both from Acros), and dried at 60 °C. 9-Fluorenone was purchased from Sigma Aldrich and used as received. Imidazole was obtained from Prolabo. 1-(4-Hydroxy-3,5-dimethylphenyl)-1-phenyl-2-ferrocenylbut-1-ene (**3**) was prepared according to previously reported procedures detailed in ref. [17].

Apparatus: Both preparative electrolyses and voltammetry were performed with an EG&G-Princeton Applied Research 2273 PARSTAT potentiostat driven by Powersuite electrochemical software. All potentials are referred to a saturated calomel electrode (SCE). ^1H NMR spectra were recorded on a Bruker spectrometer (200 MHz). EPR spectra were recorded on a Bruker Elexsys E500 X band spectrometer with a SHQ001 resonator mounted with an Oxford ESR 900 cryostat.

Procedure for the electrolyses: Preparative electrolyses were carried out in acetonitrile under an argon atmosphere in a $2\times5\ cm^3$ two-compartment cell with a no. 4 porosity sintered glass separator. The anodic compartment was equipped with a gold grid anode ($1\ cm^2$) and a SCE reference electrode, whereas the cathodic compartment was fitted with a stainless steel grid cathode. The compartments were filled with acetonitrile containing $TBABF_4$ at $0.1\ mol\,L^{-1}$ (5 mL). Compounds **1–3** (0.25 mmol) were introduced in the anodic compartment and 9-fluorenone (0.25 mmol) was introduced in the cathodic compartment to provide a reproducible and easy auxiliary cathodic reaction. The anode potential was set at +0.7 V/SCE during the electrolyses.

To follow the electrolytic process using EPR, aliquots (100 μL) of the anodic compartment were collected at selected times and introduced into an EPR tube purged with argon and were immediately frozen and stored in a container cooled with liquid nitrogen. EPR spectra were then recorded in the same sealed tubes of frozen solution. Imidazole was added directly to the EPR tube of the frozen solutions containing $\mathbf{1}^{\bullet+}$, $\mathbf{2}^{\bullet+}$, and $\mathbf{3}^{\bullet+}$. The tube was warmed just enough to allow the liquids to mix and was then immediately re-frozen for EPR recording (see Figure 4).

EPR conditions: EPR spectra were recorded on a Bruker Elexsys E500 X band spectrometer with a SHQ001 resonator mounted with an Oxford ESR 900 cryostat. Unless specified, all EPR spectra have been recorded at 20 K, with a microwave power of 20 mW, and a modulation amplitude of 0.3 mT.

NMR spectroscopic characterization of 3 and 3d: Both ^1H and ^{13}C NMR spectra of **3** and **3d** (the latter being obtained by electrochemical oxidation of **3**) fit the description of the authentic compounds.[17]

